Phase Contrast Imaging for Wendelstein 7-X

Applicant/Institution:
Massachusetts Institute of Technology
77 Massachusetts Avenue
Cambridge, MA 02139

Principal Investigator
Prof. Miklos Porkolab
Department of Physics
Tel 617-253-8448
porkolab@psfc.mit.edu

Administrative Contact
Jamie Goldberg
Office of Sponsored Programs
Tel 617-253-6287
jrgold@mit.edu

Subaward Applicant/Institution:
SUNY Cortland
22 Graham Avenue
Cortland, NY 13045

Subaward Investigator
Asst. Prof. Eric Edlund
Department of Physics
Tel 607-753-5697
eric.edlund@cortland.edu

Administrative Contact
Thomas Frank
Office of Research and Sponsored Programs
Tel 607-753-2511
thomas.frank@cortland.edu

Funding Opportunity Announcement Number: DE-FOA-0001811
PAMS Preproposal Number: PRE0000012342
DOE/Office of Science Program Office: Office of Fusion Energy Sciences
DOE/Office of Science Program Office Technical Contact: Dr. Samuel J. Barish

Contents

Phase Contrast Imaging for Wendelstein 7-X

1 Introduction

This proposal is a renewal of the project originally titled "Phase Contrast Imaging for Wendelstein 7-X" which was funded under grant ID 0000214949. The main objectives of the original proposal were to design, fabricate, install and operate a phase contrast imaging (PCI) diagnostic for the Wendelstein 7-X (W7-X) stellarator. All objectives of the original proposal have all been met within the proposed timeline and the PCI diagnostic is currently operating at W7-X in the OP1.2a campaign.

The focus of the PCI-related work until the time of writing this proposal has been development of the hardware systems and control interfaces, and data collection since the beginning of the OP1.2a campaign. The next several months will focus on continued data collection and development of more sophisticated analysis tools for examining the PCI measurements of plasma fluctuations. This suite of tools will include elements such as calculations of correlations between various diagnostics, frequency-wavenumber analysis of PCI data, absolute calibration methods, and flux surface mapping of pitch angles for localization of fluctuations.

With an operational PCI diagnostic in-place and making routine measurements of plasma fluctuations, this proposal seeks to extend into the start of the W7-X OP2 campaign . Four major elements comprise this proposal: continuation of operation through the end of the OP1.2b campaign (fall 2018), analysis of accumulated PCI data and associated numerical modeling projects, preparations for OP2, and operation of the PCI diagnostic during the first part of the OP2 campaign in 2021.

The last proposal funded MIT exclusively through Professor Miklos Porkolab as PI with Dr. Eric Edlund as lead project scientist. In the coming proposal there will be a restructuring of the organization as Dr. Eric Edlund is now employed as an assistant professor at SUNY Cortland where he will be operating as a subcontractor to the award. In this role he will support the data analysis work and development of new hardware from SUNY Cortland. A postdoctoral researcher hired through MIT will also perform data analysis, provide continued on-site support for the PCI diagnostic, and will take the lead on preparing the hardware for the OP2 campaign.

1.1 The role of fluctuation diagnostics in the W7-X experimental program

H-mode operation in stellarators, achieved with diverted magnetic geometry and auxiliary heating, shares many similarities to the H-modes observed in tokamaks, including reduced fluctuations, increased density, the possible presence of edge-localized modes (ELMs) and reductions in edge D_α emission [1]. Unlike tokamaks where the density limit is set by edge physics possibly relating to turbulence, impurity radiation [2] or magnetic island formation [3], the density limit in stellarators seems to be set by radiative losses in the core, which are the result of ambipolarity and the large, negative electric field that tends to trap impurities [4]. Thus, impurity generation and transport from the edge to the core are major issues confronting long-pulse, high-performance stellarator operation. Understanding the impact of turbulence, global transport properties and ELMs on

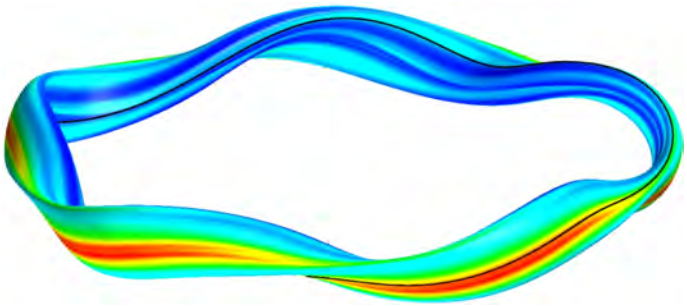

Figure 1: A flux-tube simulation of ITG fluctuation amplitude on a rational magnetic surface in W7-X shows the strongly ballooning nature of these fluctuations. Color indicates magnitude of the potential fluctuation, increasing from blue to green to red. Image provided by P. Xanthopoulos (IPP-Greifswald).

divertor heating, and the subsequent impact of impurities on core transport is a major component of establishing compatible core-edge solutions.

One of the leading candidates for advanced operation in W7-X is the high-density H-mode (HDH) regime discovered on Wendelstein 7-AS (W7-AS), coupling high density and low impurity confinement, leading to a roughly factor of 2 enhancement of the energy confinement time [5]. The physics regulating the transition to HDH is poorly understood and, similar to H-mode regimes in tokamaks, is most likely related to shear-flow stabilization of turbulence near the last closed magnetic surface (LCMS). In HDH operation it was found that the radiated power all but vanishes from the core. The authors of Ref. [5] found a complicated relationship between the energy confinement, separatrix density, and radiated power, noting that the confinement time decreased above average densities of approximately 3×10^{20} m^{-3} in higher-power discharges in W7-AS. Edge fluctuations, or in the case of H-Modes, possibly ELM events, may lead to transiently large heat loads. The performance of the divertor in managing the heat flux, recycling, and the ensuing impurity generation, are important feedback paths that will affect ability to control the profiles and manage turbulent transport. One of the concerns raised by the W7-AS studies is that the impurity screening seemed to deteriorate at higher densities with the development of a partially detached divertor plasma, raising questions about the viability of this regime in W7-X plasmas [5].

A point of significant departure between tokamak and stellarator transport is that the former exhibit strong profile-stiffness while the latter do not. In stellarators, on-axis heating with ECRH tends to drive very peaked temperature profiles and possibly somewhat hollow density profiles, while off-axis heating promotes flatter temperature and density profiles, unlike tokamak experiments that exhibit less tendency to variation. Perturbation studies using auxiliary heating have shown that neoclassical-transport-dominated stellarators tend to have thermal diffusivities (χ) that are largely independent of the temperature gradients [6, 7]. Interestingly, studies of varied magnetic geometry in stellarators, from centrally decreased to centrally increased rotational transform, or ι, via external current drive, found that there was little effect on the global confinement and turbulent properties of these plasmas [8].

The scaling of the energy confinement time for stellarators ($\tau_{\mathrm{E}}^{\mathrm{ISS04}} \sim n_{\mathrm{e}}^{0.54}$) has a much stronger dependence on density compared to tokamaks, and suggests a fundamentally different nature of

the underlying transport processes, at least for neoclassical-transport-dominated stellarators [9]. Whereas the contributions of neoclassical transport are thought to be well understood for a given a magnetic geometry and equilibrium, the spatial structure and amplitude of turbulent fluctuations, such as ITG or TEM turbulence, are comparatively poorly understood for stellarators [10, 11]. Current state-of-the-art codes, such as GENE [12, 13], calculate saturated amplitudes of ITG turbulence in the reduced problem of flux-tube geometry (as in Fig. 1) and find a significant fluctuation amplitude in high performance plasmas, though how this turbulence will affect global energy and impurity transport is not yet known. While it may be that W7-X experiments will achieve a degree of optimization such that turbulent transport is dominant, recent numerical studies of variations in magnetic geometry indicate that it may be possible to produce magnetic configurations with the existing W7-X coils that have both low neoclassical transport and suppressed levels of turbulent transport [14]. Large changes in the nature of the turbulent fluctuation spectrum have been observed to accompany the transition to H-mode in W7-AS, and point toward this subject as an area of critical research for future studies [15, 16]. Quantitative measurement of turbulence and its impact on overall performance as magnetic geometry, auxiliary heating and density are varied will comprise an integral component of developing operating scenarios for high performance plasmas that are compatible with divertor heat loads in long-pulse experiments.

1.2 The phase contrast imaging technique

The phase contrast imaging technique is an interferometric method using an internal reference beam [17, 18]. An incident laser beam is expanded, collimated and passed through the plasma to be collected on the far side. Interaction of the incident beam with modulations of the electron density from plasma waves results in small-angle scattering at an angle equal to $\lambda_0/\lambda_\mathrm{p}$, where λ_0 is the wavelength of the incident beam, and λ_p is the wavelength of the plasma waves normal to the incident beam's Poynting vector. The image intensity is a function of $\Delta = \lambda_0 r_\mathrm{e} \int \tilde{n}_\mathrm{e}\, dz$, the line integral of the electron density fluctuations along the beam path, where r_e is the classical electron radius ($\approx 2.8 \times 10^{-15}$ m) and $\tilde{n}_\mathrm{e}$ is the fluctuation in the electron density. For parameters typical of magnetically confined plasmas Δ is typically of order 10^{-2} or less. Importantly, the the scattered components of the laser beam acquire a mean phase shift of $\pi/2$ relative to the incident beam which, if no further action were taken, would not create a detectable image. However, the phase contrast technique takes advantage of the spatial separation of the unscattered and scattered components at a Fourier plane of the optical system. There, the phase of the direct beam is advanced by $\pi/2$ by focusing it into a $\lambda/8$ groove on a "phase plate", modifying the relation between the unscattered and scattered components in the final image to

$$I_\mathrm{PCI} \approx E_0^2 \left| i + i\Delta \right|^2 = E_0^2 \left(1 + 2\Delta + \mathcal{O}\left(\Delta^2\right)\right). \tag{1}$$

The phase contrast method provides a simple correspondence between the image and density fluctuations since the response is linear in Δ and therefore proportional to $\int \tilde{n}_\mathrm{e} dz$. The phase contrast technique is rather insensitive to errors in equilibrium reconstruction, and plasma motion enters into the signal as a simple Doppler shift. Absolute calibration of the density fluctuations measured by PCI is performed by measuring the fluctuations induced by small changes in the index of refraction of air when sound waves of known intensity are launched across the path of the PCI laser beam on the transmitting table.

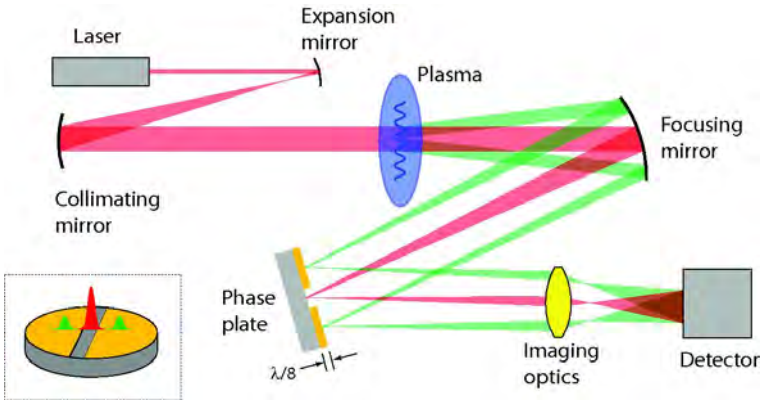

Figure 2: Scattered waves are manipulated at the Fourier plane with a phase plate, which adds a phase factor of $\pi/2$ to the unscattered component, yielding an image whose intensity is linear in the density fluctuations.

The main complication in the measurements is the interpretation of the line-integrated nature of the fluctuations, which naturally leads to a "synthetic diagnostic" approach implemented in codes. While the PCI measurements themselves constrain the absolute fluctuation levels, it is possible that phase cancellation effects resulting from summing positive and negative density fluctuations reduce (or possibly enhance) the apparent magnitude of the density fluctuations, as is especially present in measurement of MHD modes. However, the spatial structure of the integrated fluctuations is quite sensitive to the 2D structure of the fluctuations and contains enough information that the radial location of coherent modes can be constrained [19].

The output signal from the detector can be converted to a measure of integrated electron density fluctuation through a calibration against a known perturbation source. As in prior PCI diagnostics, the W7-X system uses a sound wave launched from a speaker to provide a density perturbation in air that simulates scattering from plasma waves. Once the sound wave structure and amplitude has been measured it is in principle possible to back out the calibration factors needed to scale the PCI signal to absolute line-integrated electron density fluctuation.

1.3 Summary of progress during 2015-2017

Under the current grant, preliminary design activities began in earnest after initial funding in the summer of 2015. Multiple design reviews were conducted at IPP-Greifswald and at MIT in the winter and spring of 2016, leading to a final design plan in the summer of 2016, at which point acquisition and fabrication began. The design of the W7-X PCI system was presented at the 2016 APS conference [20] and experimental results from the OP1.2a campaign were presented at the 2017 APS conference [21].

The first hardware shipments were delivered to IPP starting in November of 2016, with the majority arriving in January and February of 2017. Initial setup of the optics and laser took place in a dedicated laser lab at IPP and in May 2017 the optics tables were transferred to the Torus Hall (TH) for final installation. This work continued throughout the summer, with final commissioning

tests on September 2, 2017. The PCI diagnostic has been operating throughout the fall 2017 campaign except for a three week period during which the laser power supply was being repaired.

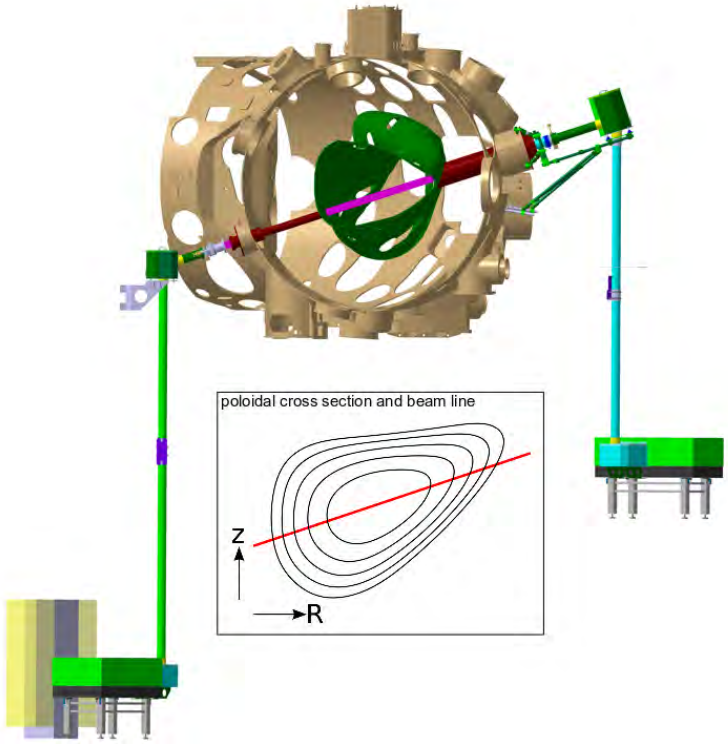

Figure 3: CAD drawings showing the PCI beam path from the inboard AEZ-50 port to the outboard AET-50 port in module 5. The PCI system is located in module 5 at a toroidal angle of 112°.

1.4 Overview of the W7-X PCI diagnostic system

The W7-X PCI system has two main optical tables, one that houses the lasers and is referred to as the transmitting table, and the other that has the detectors and is called the receiving table 3. Two intermediate mirror boxes provide the beam steering through the system. Some of the major design elements of the system are described in the following paragraphs.

1.4.1 Transmitting table

The transmitting table houses the two lasers used in our system and the required optics for beam preparation and steering. The overall optical design is largely determined by three primary considerations.

The first is that the source laser for measurements, a 100 Watt CO_2 laser operating at 10.6 μm, requires careful handling due to the human hazards involved in its operation. W7-X operating policies have declared that the TH must be closed to all but a small set of authorized personnel

when the CO_2 laser is operated during testing and alignment phases. This aspect of operation necessitates the use of a Class 2 visible laser, in our case a HeNe laser, so that the majority of the alignment checks can be completed without a TH closure.

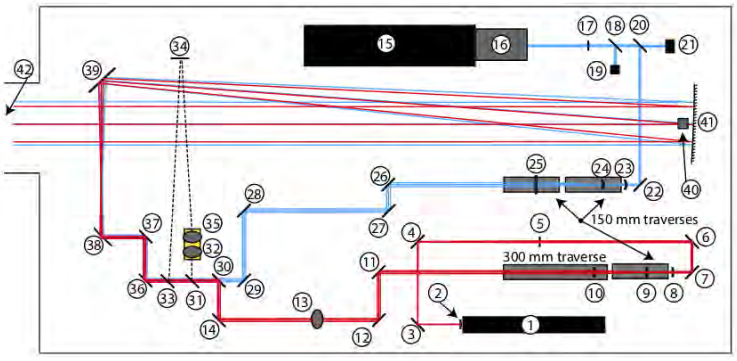

Figure 4: Layout of the transmitting table optics, including lenses, mirrors, lasers and observation targets. The blue lines represent the CO_2 laser beam and the red lines represent the HeNe laser beam.

The second design consideration is the need to expand the laser from its initial approximately 2 mm beam width to a beam size of approximately 120 mm. It is not possible to have proper collimation of both beams with a lens-based system due to the difference in the index of refraction at visible and IR wavelengths. Therefore, each laser passes through its own first stage lens-based telescope, and then after the two lasers have been combined, they jointly pass through a second mirror-based telescope for final expansion to large diameter. Each telescope is composed of three lenses, two of which are mounted on linear stages to allow for variable magnification to change the final beam size. The secondary telescope is composed of two off-axis parabolic mirrors with a total magnification of 80”/6” = 13.3 that provides the final expansion of the laser beams to the large diameter necessary for plasma viewing.

The last design consideration is that remote controllable optics are required because the TH may be closed for periods of up to three days during OP1.2b, due to the desire to minimize the number of cycling stresses from ramping the magnetic field. Any changes in the optics arising due to thermal drifts or vibrations can be fully counteracted with the system of two-dimensional steering mirrors that is in place.

1.4.2 Mirror boxes

After leaving the transmitting table the beam passes through a series of three 9” diameter steering mirrors to reach the inner (AEZ-50) port assembly. Two these three mirror mounts have been fitted with remotely controllable piezo-inertial motors for tip-tilt steering.

After passing through the vacuum vessel the beam passes out of the AET-50 port to the outer mirror box that houses an additional two steering mirrors. Between these mirrors is a an array of 50 ultrasonic transducers that launch 43 kHz pressure waves that cause the beam to scatter. In principle, this scattering mimics the scattering from plasma and allows determination

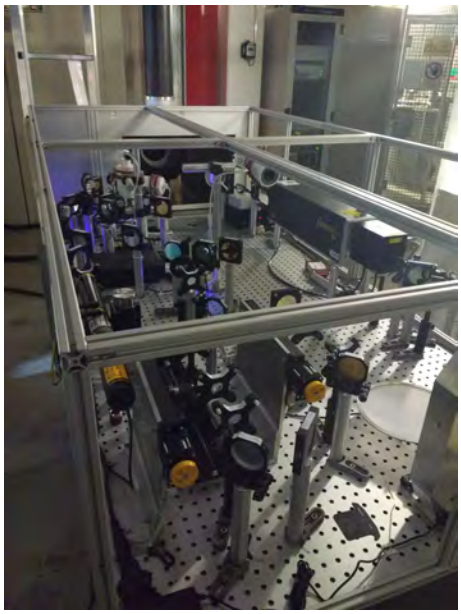

Figure 5: Photo of the transmitting table installation. The CO_2 laser can be seen on the right hand side of the table, the 9" diameter off-axis parabolic mirror at the bottom right (clipped), and the first 9" diameter steering mirror just visible at the far end of the table.

of the calibration factors from which the absolute density fluctuation level can be determined. In practice, this is a difficult measurement and the existing hardware has proven insufficient for reliable measurement of these properties.

After leaving the outer mirror box the laser beam is directed downward to the receiving table where it is reflected off of two 9" diameter steering mirrors before reaching the 9" diameter OAP mirror that is the first element of the condensing telescope. One of the 9" diameter mirrors in the outer mirror box and one on the receiving table are also fitted with piezo-inertial motors for tip-tilt steering.

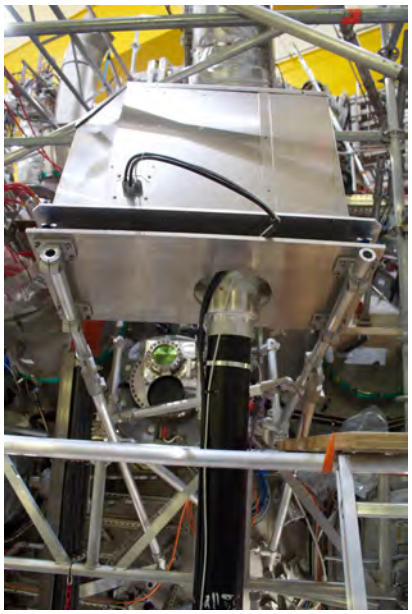

Figure 6: Photo of the outer mirror box that houses two 9” diameter steering mirrors and the sound wave calibration system. The beam on the bottom of this mirror box connects to the receiving table. The ZnSe window at the beam line exit of the AET-50 port can be seen in the photo just below the mirror box, to the left of the beam duct (normally covered by an additional beam duct during operation).

1.4.3 Receiving table

The receiving table houses the phase plate (the essential optical component for the phase contrast technique), the telescopes and optics for image generation, the masks for isolation of wavenumber components, and the detectors. A synopsis of some of the major components are described in the following paragraphs.

Final image generation at the detectors is produced by means of a two-stage telescope system, similar to that used on the transmitting table. The first stage is composed of two OAP mirrors that produce a net magnification of 6”/80” = 0.075, with the phase plate located at the focal plane between them. The second telescope assembly is composed of a three-lens system, with the latter two lenses mounted on remotely controllable linear stages that allow for a variable magnification at the detector, which allows the measured k range to be optimized for long wavelength or short wavelength detection. The achievable magnifications with the current optics are in the range of about 1 to 5. This means that a 100 mm beam through the plasma is imaged at the detector with final image sizes between 7.5 mm and 37.5 mm. Together with the wavenumber filtering provided by the phase plate, the adjustable telescopes provide a minimum and maximum wavenumber range of about 0.5 cm^{-1} to 23 cm^{-1}. Because of the relatively long focal lengths used in the second stage telescope, a good depth-of-focus is created at the detectors, meaning that the system is fairly robust to small imperfections in optical positioning.

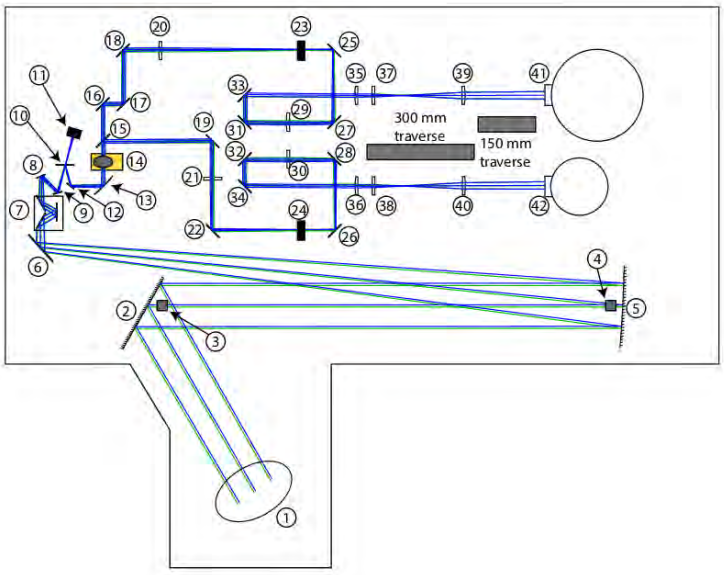

Figure 7: Layout of the receiving table showing the beam entering the table on the extension, passing through the image rotator (element 7), passing to the phase plate (element 10), beam splitter (element 15), passing through the rotating masks (elements 23 and 24), and on to the detectors (elements 41 and 42).

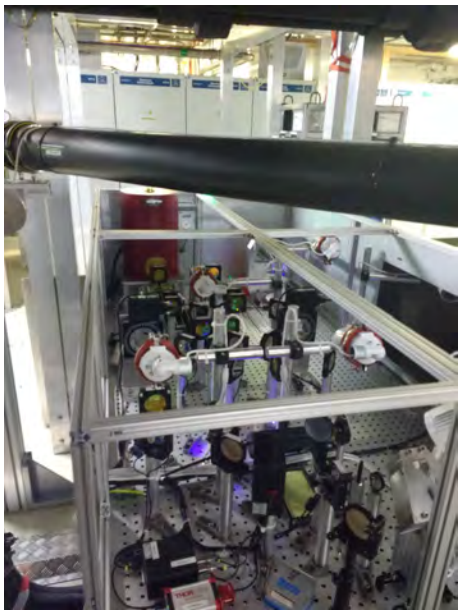

Figure 8: Photo of the receiving table installation. The detector can be seen at the rear-left side of the optics table. The black object above the table is the Thomson scattering beam duct.

A series of three flat mirrors prior to the phase plate creates an image rotator that allows the image of plasma fluctuations to be rotated at an arbitrary angle. This device, shown in figure 9, is used to align the direction parallel to the central magnetic field with the axis of the detector. If left uncorrected, the image of the plasma fluctuations would have the $\vec{B}_{||}$ direction nearly aligned along the detector array, meaning that little of the fluctuations propagating perpendicular to the magnetic field would be detectable. The image rotator is set to create an image with $\vec{B}_{||}$ on-axis exactly perpendicular to the array.

Figure 9: In the left figure is the three-mirror image rotator that can be set at an angle between 0° and 90°. The right image shows the rotation of an MIT ID card when the image rotator is set to an angle of approximately 60 degrees, the output image is rotated by approximately 30 degrees.

The beam path is split into two paths following the second OAP on the receiving table, leading to two detectors, each with an independent mask system. Each mask selects for fluctuations from a range of flux surfaces in the plasma based on the local magnetic pitch-angle of the plasma. With two detectors and independent masks, it is possible to simultanously observe two different regions in the plasma, which adds the possibility of deriving radial correlations of fluctuations. The second detector is with the manufacturer (Infrared Associates) for repair and will arrive prior to the start of the OP1.2b campaign. The plan under the current funding cycle is to continue to operate the diagnostic through August 15, 2018.

1.5 PCI measurements from the OP1.2a campaign

With the exception of a three week period where the CO_2 laser was not functioning because of failure of the RF amplifier, the PCI diagnostic has collected data in every run week. While there has been little time to stop and analyze the date carefully at this time due to the continued need to maintain the system and attention given to developing data analysis and control software, there now exist a range of observations that deserve further attention. Some of these are described in the following subsections.

1.5.1 Alfvénic modes

A series of coherent, frequency chirping modes have been observed in some W7-X experiments with an early transient dip in the electron density (Fig. 10). The frequency of these modes first increases, in accordance with the Alfvén frequency calculated using the line-integrated electron density measured with the single-chord interferometer, then appears to decrease briefly and slowly rise again. This scaling with density suggests that these modes may be Alfvén eigenmodes. While the absence of any ion heating on W7-X means that there are certainly no energetic ions to excite these modes, it is possible that the low density conditions of the early plasma phase together with significant ECRH may be sufficient to generate a substantial fast electron distribution that could excited these modes. Further comparisons with Mirnov coil data and reflectometer data are underway. These modes along with observations of broadband fluctuations were reported and discussed at the IPP science meeting on November 27, 2017.

It is speculated that these modes are perhaps similar to the reversed shear Alfvén eigenmodes that were observed during the current ramp phase of Alcator C-Mod plasmas with early ICRF heating, as shown in Fig. 11. There, the fast ion population, generated by ICRH, that formed in the relatively low density phases of these plasmas was responsible for excitation of the RSAEs. The increase in frequency arises because the eigenmode frequency scales like $k_{||}$, which is proportional to $m\iota_{max} - n = m/q_{min} - n$. As the q profile relaxes during the transient current diffusion phase, $k_{||}$ increases as q_{min} decreases, causing the frequency of these modes to increase rapidly.

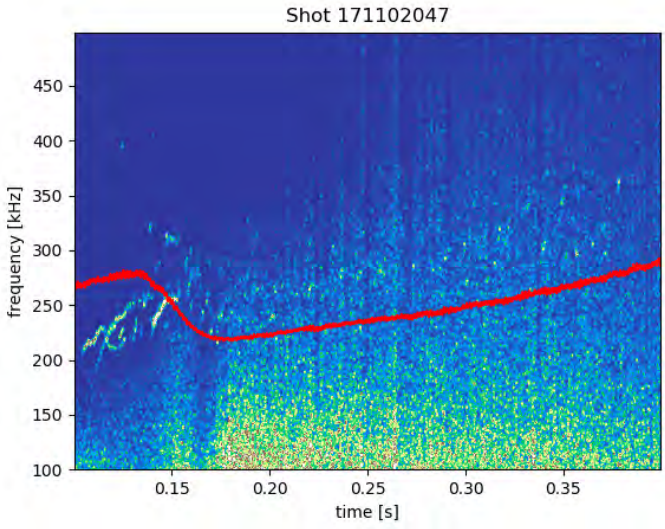

Figure 10: PCI measurements of electron density fluctuations from program 20171102.047 showing coherent modes in the range of 200-250 kHz that are excited during the early part of the experiment between 100 and 150 ms. The red overlay trace is proportional to the Alfvén velocity. Weaker bursts of these modes can be seen later in the program, generally following the Alfvén frequency.

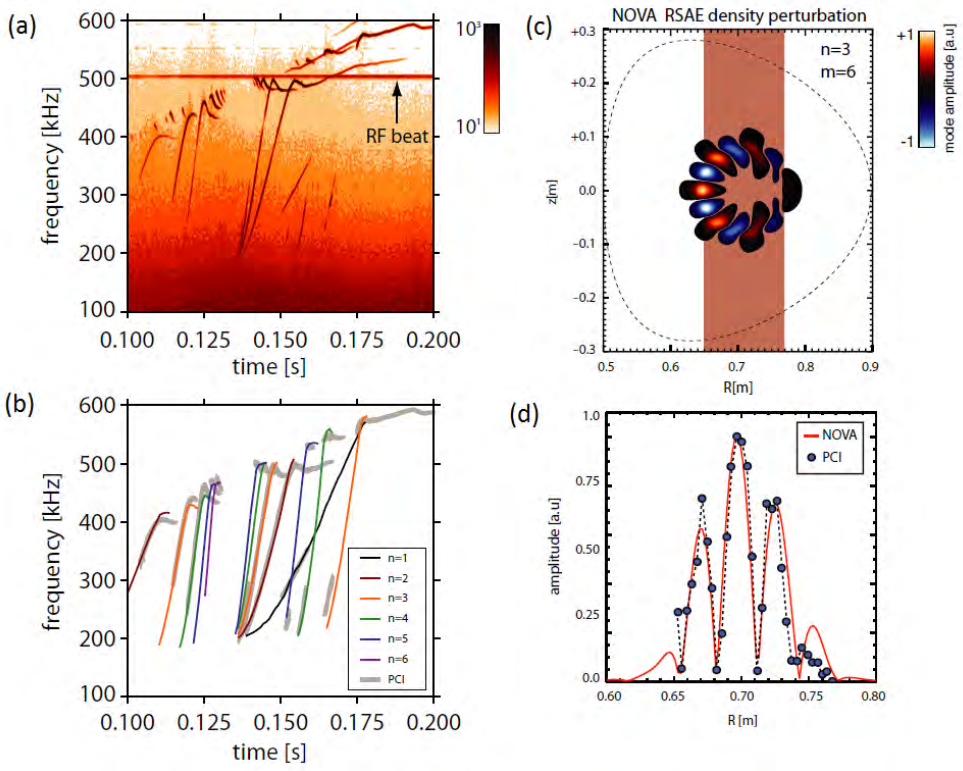

Figure 11: Figure taken from Ref. [22] showing (a) PCI measurements from Alcator C-Mod experiments where a series of RSAEs are excited by energetic ions created by ICRF heating during the current ramp, (b) modeling results from NOVA, (c) 2D plot of the for an $n = 3$ RSAE, and (d) comparison of the mode structure for the $n = 3$ RSAE measured by PCI to that calculated with a synthetic diagnostic analysis based on the NOVA modeling.

1.5.2 Broad-band turbulence

Broadband density fluctuations that are generally associated with the nature of the confinement regime typically increase nearly proportional to the background density, as in Fig. 12, within a given confinement regime. As prior experiments in tokamaks [23–25] and Wendelstein 7-AS [16] have shown, transitions in the nature of the broadband turbulence are highly correlated with transitions in the confinement regime, often with H-mode type confinement exhibiting lower fluctuation levels.

The data presented in Figs. 12 and 13 compare two shots with similar heating and density characteristics, differing only in that the former was conducted in helium and the latter in hydrogen. As can be seen in the PCI spectra, the turbulence spectra in these cases is wildly different, both in amplitude and in the spectral shape of the fluctuations, with the helium plasma showing a much broader range of fluctuations. This may be due in part to the difference in H and He transport, but is more likely due to the difference in the profile shapes that arise from the different fueling methods, thereby differently exciting ITG and TEM fluctuations in the higher density regimes.

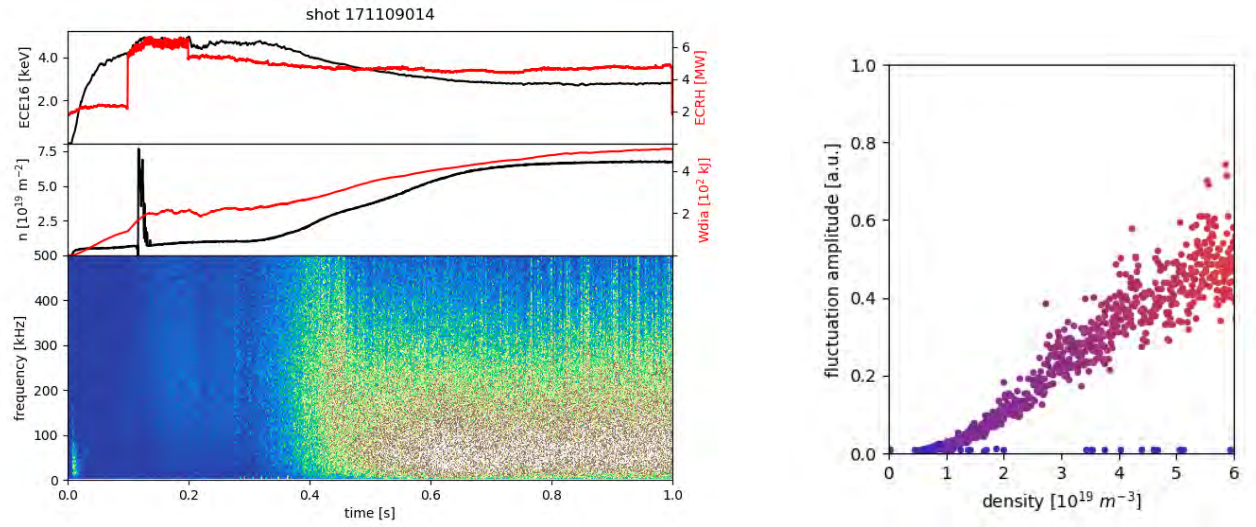

Figure 12: PCI measurements of electron density fluctuations in a helium plasma. The topmost plot on the left presents a core ECE channel in black and the total ECRH heating power in red, the middle plot presents line-integrated electron density in black (from the single-channel interferometer) and stored energy in red, and the bottom plot is a spectrogram of PCI data. The plot at the right shows the integrated density fluctuation (10-200 kHz) level plotted against line-averaged background density with time progressing from purple to orange.

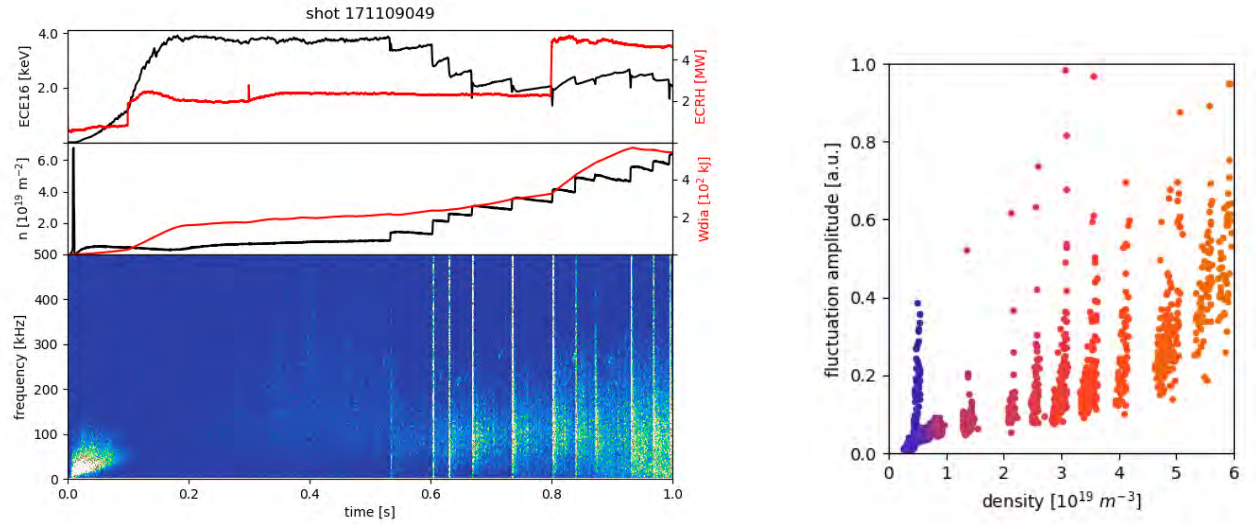

Figure 13: Similar to Fig. 12 except in a pellet-fueled H plasma.

1.5.3 Low-frequency quasi-coherent modes

Occasionally a large amplitude, low-frequency series of quasi-coherent modes are observed, often during abrupt transitions as the ECRH is switched off, as for example in Fig. 14. The mode frequency tends to scale with a positive power of the mean density, suggesting that these modes are not Alfvénic in nature, but may instead be a rotating island that is slowing down as the plasma rotation decreases.

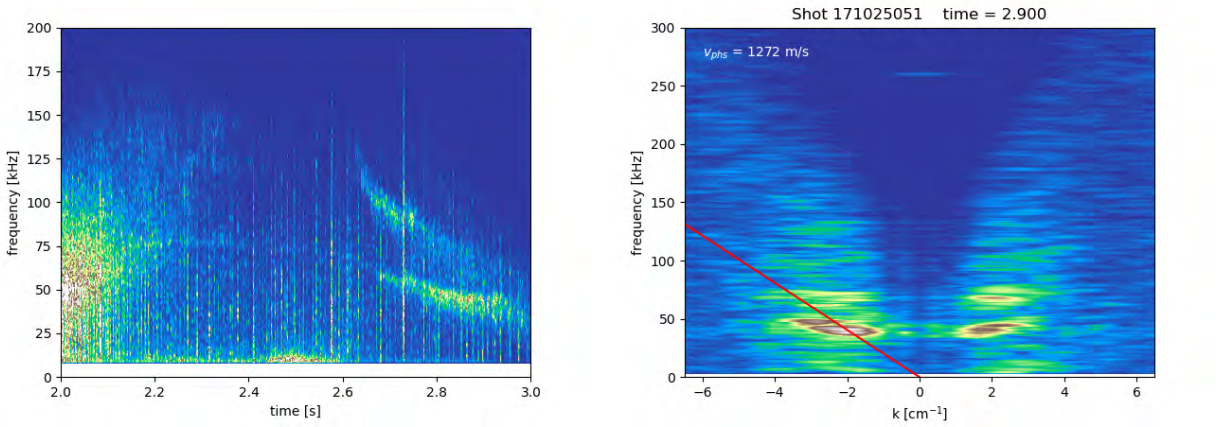

Figure 14: PCI measurements of electron density fluctuations from program 20171025.051 showing frequency down-chirping modes after the ECRH is turned off around 2.7 seconds. Shown at right is the wavenumber spectra that identifies the mode as having a dominant negative wavenumber component with a phase velocity of about 1.3 km/s. While the second harmonic of the mode is clearly visible in the frequency-time spectrogram, the wavenumber analysis indicates the presence of a third and fourth harmonic.

1.6 Experimental proposals submitted

Two experimental proposals have been submitted to the W7-X experimental program committee. The first, titled "Impact of ion dilution on ITG turbulence" with Miklos Porkolab as first author, seeks to explore the variations in fluctuation levels when the plasma is seeded with impurity ions of intermediate mass elements like neon or nitrogen. By diluting the main ion species the ion-temperature gradient (ITG) modes are expected to diminish in amplitude. This subject has important consequences beyond the obvious connection to tests of turbulence codes since it is expected that some amount of edge impurity seeding will be necessary to create a radiative divertor in high-performance plasmas and some of these impurities will naturally enter the core plasma.

The second proposal, titled "Modification of TEM drive density profile variation using pellet injection" with Eric Edlund as first author, seeks to exploit the pellet injection system to modify the density profile as a means of modifying the stability of trapped-electron mode (TEM) turbulence. This proposal was selected for run-time in OP1.2a, though it has yet to be scheduled due to delays in the availability of reliable profile measurements.

2 Proposed Research

The PCI diagnostic method is capable of detecting a broad range of modes, including turbulent fluctuations [23, 26, 27], edge turbulence associated with transitions in confinement [28], coherent Alfvénic waves [19,22], mode-converted ICRF waves [29,30] and a range of MHD activity [31]. The proposed research of this proposal seeks to use the PCI diagnostic to generally examine plasma phenomena of interest.

The FOA to which this proposal responds has identified five major areas of research interests for the W7-X program. These are: (1) core-edge solutions, (2) plasma-divertor interface, (3) exploitation of US hardware investments, (4) long pulse and high power operation, and (5) comparative studies between LHD and W7-X. The main thrust of this proposal is continuation of experimental studies using the new PCI system that was implemented on W7-X under US DOE funding, addressing topical area 3. In terms of physics, we will examine the effect of plasma turbulence and coherent modes on energy and particle transport, thereby addressing topical area 1, 2 and 4.

In particular, the emphasis on topical area 3 will examine turbulent transport through comparisons of the measured fluctuation levels with variations in plasma conditions and magnetic geometry that are theoretically predicted to modify the stability of ITG, TEM and possibly the electron-temperature gradient modes (ETG). Recent work by Xanthopolous *et al.* [32] has shown that the ITG mode is expected to peak on the outboard side of the plasma, and should be detectable with PCI. Additionally, recent work by Proll *et al.* [33] has shown that variation of the mirror ratio can affect the linear growth rate of the spectrum of trapped electron modes. They speculate that the change in the linear growth rate will manifest as a change in the saturated amplitude of the turbulent TEM spectrum.

With the addition of neutral beam injection (NBI) and ion-cyclotron resonance heating (ICRH) that are currently scheduled for OP1.2b, there will be a significant programmatic interest in the physics of Alfvénic modes and energetic ion transport. This subject is intimately tied to topic areas 1 and 2 where additional heating will modify the core temperature profiles, thereby affecting global transport which will in turn affect divertor heat loads. Additionally, losses of energetic ions from mode-induced transport [34] may also become a serious concern for long-pulse operations with a heating scheme that combines ECRH, ICRH, and NBI.

The next sections describe this proposal's contributions to four four major areas of research over the three-year period beginning in August 2018. These areas are: (1) operation of the PCI diagnostic during the end of the OP1.2b campaign, (2) data analysis of OP1.2 data, which includes code development and, time permitting, running of nonlinear gyrokinetic codes for turbulence modeling, (3) hardware modifications for in OP2, and (4) operation of the PCI diagnostic in the beginning phase of OP2 scheduled for the spring of 2021.

2.1 Diagnostic support through the end of OP1.2b

The OP1.2b campaign is scheduled to begin in April, 2018 with pump-down and leak testing of the W7-X cryostat and vacuum vessel. Based on experience from preparations for the OP1.2a campaign, this phase took about two months to complete before field line mapping could begin.

Thus, the current schedule places the start of physics operation at July 11, 2018. The OP1.2b campaign will continue for about four months, well beyond the end of the current funding cycle (ending August 15) and into the first year of the first year funding phase covered by this proposal.

Dr. Eric Edlund will participate in summer activities up until mid August, essentially to the end of the current funding cycle, but will have to return to the US after that to resume teaching duties at SUNY Cortland. The new MIT postdoctoral researcher starting in January, 2018 will then continue operation of the PCI diagnostic into the fall and through the end of the OP1.2b campaign. Duties during this period include regular maintenance and operation of the PCI diagnostic during campaign, analysis of data, and presentation of results for colleagues and scientific conferences.

2.2 Data analysis and development of a synthetic PCI analysis and other tools

With W7-X operating typically 60 experimental programs per day, a large amount of PCI data has been accumulated during the OP1.2a campaign to-date. The daily tasks of operating and maintaining the diagnostic means that the PCI team cannot simultaneously process and analyze all of the PCI data that is available. This means that a concerted effort to review all of the data acquired during the OP1.2a and OP1.2b campaigns will be an ongoing task that will span the entirety of the funding period. The data analysis tasks will focus on four main subareas: development of analysis codes and synthetic diagnostic calculations, analysis of turbulent fluctuations, analysis of Alfvénic activity, and analysis of programs of interest for collaborators.

While a core set of PCI data analysis codes currently exists, there are many additions that could be implemented. In particular, analysis tools to calculate cross correlations with other diagnostics (e.g. Mirnov coils and ECE diagnostics) and cross-phase analysis for identification of nonlinearly coupled modes will be developed to enhance the depth of commentary that can be made on a wide range of plasma waves. Additionally, a graphical-user-interface will be created and disseminated to enhance access of all W7-X scientists to PCI data.

Comparison of PCI measurements to calculations from codes involves some amount of transformation of the data from one representation to the other. Because the PCI measurements are integrals of density fluctuations along chords through the plasma, it is generally not possible to identify local fluctuations in the plasma. Instead, the typical approach is to take the density fluctuation calculations from simulations and forward those model to generate a "synthetic PCI" calculation that includes the line-integration and diagnostic response functions [35]. This type of forward modeling is non-trivial and typically involves interpolating numerical calculations (often calculated in flux surface coordinates) onto a cartesian grid for volume integrating. Development of a generalized synthetic diagnostic package that performs the integration of signals and includes the diagnostic response that can accept any fluctuation input will be begin in year 1 of the proposal.

2.3 Preparations for OP2

The work packages for OP2 preparations of the PCI system include redesign of a significant amount of the existing optics on the transmitting side, new optics for beam steering to the inboard port, improved calibration techniques, and the addition of a heterodyne detection scheme for observation of ICRH waves. Each of these elements is described in greater detail in the following subsections.

2.3.1 Improved sound wave calibration

The current method of calibrating the PCI system involves measuring the diffraction of the laser signal from density variations in air that are created from a high-intensity, traveling sound wave. The sound wave calibration device that is currently installed in the W7-X PCI system operates at 43 kHz, which corresponds to a 0.8 cm wavelength in air. This calibration method is used to verify the net optical magnification by measuring the wavelength of the sound wave.

In principle, PCI measurements of the sound wave amplitude can also be used to provide an absolute calibration of the system when the absolute scale of the 3D wave field of the pressure waves is known. In practice, this analysis is difficult and fraught with inaccuracies due to the requirement to integrate the fluctuations along the beam path, which is sensitive to both absolute position of the laser beam and its angle of incidence. Additionally, one must have a complete 3D model of the real sound field, including both amplitude and phase components of the signals.

Dr. Eric Edlund will develop a new calibration system at SUNY Cortland using an alternative speaker arrangement and reflective surfaces. A set of two of calibrated microphones will be used to accurately measure the spatial structure of phase and amplitude so that an accurate 3D model of the pressure waves can be reconstructed for numerical integration from which relative and absolute calibration factors can be extracted.

2.3.2 Heterodyne detection of ICRF waves

With the installation of ion-cyclotron resonance heating (ICRH) antennas, planned for OP1.2b and onward, there will be great interest in the efficiency of this heating scheme and the generation of energetic minority ions such as H or ^{3}He. An optical heterodyne system using an acousto-optical Ge crystal will be used to frequency modulate the CO_2 laser beam near the ICRH frequency of 27 MHz. By modulating the CO_2 laser at 27.5 MHz, for example, a beat wave at 500 kHz will be detectable by the PCI detectors, which have a characteristic -3 dB frequency of about 600 kHz.

A similar system has been employed with great success on the Alcator C-Mod PCI system [30], where direct observation of mode-converted ICRF waves have been observed. These measurements provided a way to test the modeling of ICRF wave propagation with the AORSA and TORIC full-waves codes by constraining both the spatial structure an absolute magnitude of the induced density perturbations [29].

Special consideration needs to be taken to integrate the acousto-optical modulator (AOM), that provides the frequency modulation, into the optical system. Typically the heterodyne technique requires splitting the beam into a modulated and un-modulated beam path and recombining these following the AOM. The two beam lines are then recombined, resulting in a beam with a modulated amplitude at the AOM frequency. This modulated pattern then acts like a strobe light in the plasma to pick out waves near the desired RF frequency.

As a side project, the AOM can allow access to the ion-cyclotron range of frequencies in the plasma and thus may allow observation of ion-cyclotron emission [36, 37].

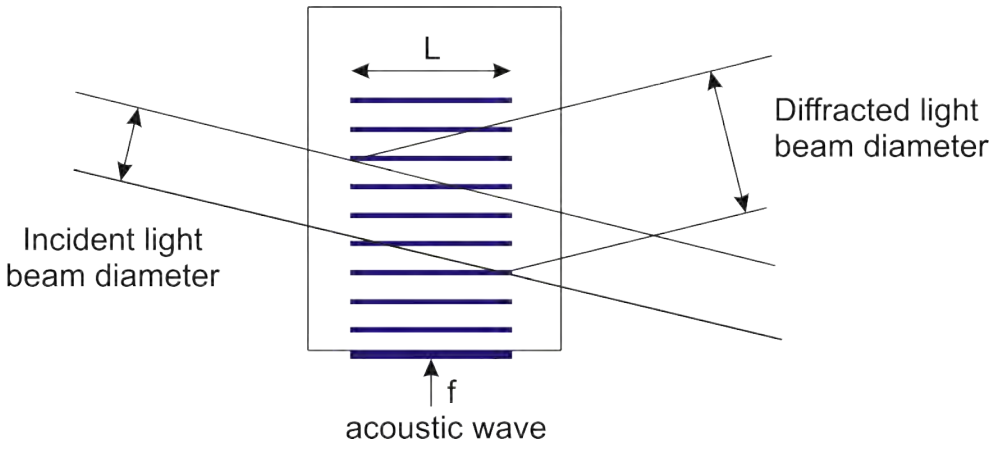

Figure 15: An acousto-optical modulator shifts the frequency of an incident beam by Bragg scattering off planes in crystal in which a compressional wave is propagating. The first order scattered beam, which in the case illustrated in the figure is frequency-upshifted, is combined with an un-modified beam to create a traveling wave with a modulation at the AOM frequency. An optical heterodyne system is created by the interaction of the modulated laser beam with a plasma wave near the modulation frequency which creates a beat wave in the frequency range of the detector.

2.3.3 Optics redesign

The current port pair (AEZ-50 & AET-50) that are being used for the PCI beam line will be available for continued use during OP2 and no changes to the core viewing geometry are expected. However, the W7-X upgrades for the OP2 campaign require the additional of another liquid nitrogen cooling system in the second basement level in the TH exactly where the PCI transmitting table currently resides. This means that the transmitting table will have to be relocated. Options for the new position of the transmitting table are currently being identified and assessed.

A consequence of the relocation of the transmitting table to any other location is that at least one, but likely two, additional mirror boxes will be required to steer the beam through the TH to the AEZ-50 port. As with the current design, each mirror box should be outfitted with gimbal-mount tip-tilt steering mirrors with remote control motors so that beam alignment can be corrected from the control room. These new components will essentially replicate what has been used elsewhere. The proposed budget includes the necessary hardware for the worst-case scenario in which two additional mirror boxes are required.

With the addition of water-cooling lines for the water-cooled divertors in preparation for long-pulse operations, the inner mirror box and associated beam ducts may have to be modified to accommodate the new space restrictions. It is anticipated that the transmitting-side beam ducts may need to be substantially reduced in size. The consequence of such reductions is that the expansion optics to create the approximately 100 mm diameter beam must be located in the inboard mirror box. Given the very limited space to work with here, a careful design review process will need to be undertaken to fit the expansion telescope into this space. It is likely that a custom off-axis parabolic mirror will need to be procured for this role, in addition to other optics.

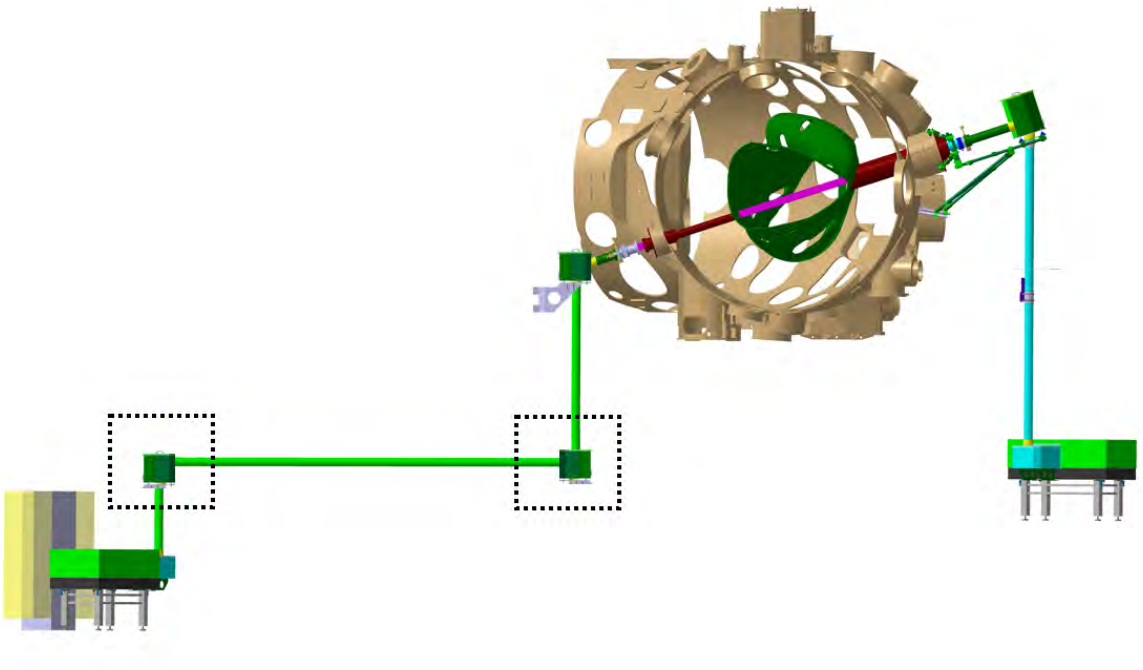

Figure 16: Conceptual design for the new layout in OP2 where the transmitting table has been relocated within the TH and two additional mirror boxes are installed for beam steering, identified in the dashed boxes (compare to Fig. 3).

2.3.4 Solid state absolute calibration development

As noted in §2.3.1, the derivation of an absolute calibration scaling that allows direct conversion between the measured detector voltages and an integrated density fluctuation in units of m^{-2} is difficult and requires very precisely measured models of the both the sound field and the beam path through the sound field. It is possible to provide an absolute calibration of the PCI system using an alternative, solid-state calibration device that eliminates the uncertainties associated with the sound wave calibration method. The additional benefits of this method are simplicity of alignment, the ability to measure the optical rotation from plasma to detector, and an extremely precise and reproducible measurement of beam quality and system performance.

The advanced absolute calibration source for the PCI system will be researched and developed by Dr. Eric Edlund at SUNY Cortland. The concept behind this new calibration technique is a precision etched window, such as ZnSe or other similar IR material. The etching pattern is a periodic series of 1-d trenches, cut with either a sinusoidally or square wave depth pattern. The variations in the thickness of the material induce local variations in the phase of the laser beam, resulting in scattering of the laser beam that emulates the diffraction from the plasma itself.

A typical phase accumulation from the laser beam passing through a high-intensity sound wave in air is about 0.2 radians. A similar phase accumulation can be generated by a change in the

thickness of a ZnSe window (index of refraction at 10.6 μm is approximately 2.4) of about 200 nm. Such depths are well within the capabilities of industrial-quality semiconductor manufacturing facilities. The radius of curvature of a 200 nm groove depth (assuming a sinusoidal depth pattern) with a wavelength of 2 cm is approximately 50 km, meaning that to all practical effects, this etching appears as a flat plate and only causes diffraction by phase shifting the beam, exactly as a phase object like a plasma.

The etched window will be carefully measured using surface profilometer or interferometric techniques so that the variations in phase induced by the etchings are accurately known. Bench tests using an old HgCdTe detector that is owned by the MIT PSFS will allow the characteristics of this calibration method to be precisely determined before introducing it into the PCI system on W7-X.

2.3.5 Diagnostic operation in OP2

The W7-X OP2 experimental campaign is scheduled to begin in the spring of 2021. The process of debugging the control software, which controls the many components of the remote control system, safety interlocks and laser power, among other things, is a dedicated project in itself. Testing of the full optical system in the TH requires closure due to considerations of personnel safety in the event of stray radiation. These tests are usually approved for evenings or weekends, and no more than once per week. As such, testing and commissioning plans leading to operations can take a significant fraction of a month. The entire installation, debugging and commissioning process is anticipated to take approximately six months to complete, meaning that this work should begin no later than September of 2020.

Daily staffing of the diagnostic during the campaign is essential for ensuring the fidelity of the data collection and for interfacing with the other diagnosticians. The MIT postdoctoral researcher will be the primary responsible person for ensuring operation during the OP2 campaign. In addition to the daily tasks of monitoring the data and operating the PCI diagnostic, it is often the case that manual adjustments to the optics are needed in addition to those that can be provided by the remotely controllable steering optics. Thus, the hardware installation and operations project is anticipated to occupy the nearly the entirety of third year for the MIT postdoctoral researchers. Dr. Eric Edlund will participate in the setup and experiments, as available.

3 Timetable of Activities and Project Objectives

The majority of the work during this contract period will be performed by a postdoctoral research (being hired through MIT at the resent time), and Dr. Eric Edlund (SUNY Cortland). Professor Miklos Porkolab will advise experimental plans and assist in research objectives from MIT. In addition, he will oversee the activities of the postdoctoral associate (located permanently in Greifswald, on-site at W7-X) via regular video conference calls and occasional site visits to Greifswald. Professor Edlund will also participate in these zoom calls from Cortland. The zoom calls may also include Dr. Olaf Grulke who coordinates local activities with the W7-X team and engineers. Prof. Porkolab will be also responsible for overseeing a career path development program for the postdoctoral fellow, as required by MIT. Finally, he will be responsible for overseeing the budget and annual progress reporting as required by DOE. He will also be responsible for quality control of publications and presentations that arise from this work. As it turns out from past experience, this job is quite time consuming.

The following tables identify the primary tasks of each group and the estimated timeline over which these activities will occur. It is assumed in these timelines that funding will be disbursed so as to allow direct continuation at the end of the present funding cycle. The annual schedules run from August 15 to August 14 of the following year, with Year 1 beginning in August of 2018.

3.1 MIT Tasks

Grant Year 1 Tasks
August 15, 2018 - August 14, 2019

Task	Period
Operate the PCI diagnostic in the OP1.2b campaign	August - October
Present OP1.2 results at 2018 APS (Portland, OR)	November 5-9
Disassemble PCI optics and hardware and remove from the TH	November - December
Assist in re-design of transmitting table optics	January - February
Continue analysis of OP1.2 data and develop synthetic PCI analysis tools	March - August
Present results at the 2019 EPS conference (TBD)	July

Grant Year 2 Tasks
August 15, 2019 - August 14, 2020

Task	Period
Attend the 2019 International Stellarator and Heliotron Workshop	September
Attend the 2019 APS conference	October
Continue development of synthetic PCI tools and data analysis	November - January
Set up optics table in IPP laser lab	February
Integrate heterodyne system and full system tests	March - April
Further data analysis & modeling	May - June
Attend the 2020 EPS conference	July
Begin installation of optics in the TH	July - August

Grant Year 3 Tasks
August 15, 2020 - August 14, 2021

Task	Period
Finalize installation of hardware in the TH	September - October
Attend the 2020 APS conference	October
Diagnostic testing & commissioning	November - January
Data analysis, modeling and synthetic PCI analysis	February
Participation in the OP2 campaign	March - August

3.2 SUNY Cortland Tasks

Assistant Professor Eric Edlund will be available to participate in research activities during the summer months between the spring and fall semesters, and approximately one day per week during the semesters. While SUNY Cortland does not have a graduate program, he will engage undergraduate research assistants in this projects to the extent allowable by funding and project scope. He will also seek outside funding as available to augment the project award to fund student summer travel to Germany to participate in experiments and research activities on-site in Greifswald. Planning for these research activities will be coordined with IPP-Greifswald.

Grant Year 1 Tasks
August 15, 2018 - August 14, 2019

Task	Period
Present OP1.2 results at 2018 APS (Portland, OR)	November 5-9
Conduct re-design of transmitting table optics to include the optical heterodyne system	November - February
Procure new hardware for heterodyne system	March - May
Setup and testing of heterodyne system	June - August

Grant Year 2 Tasks
August 15, 2019 - August 14, 2020

Task	Period
Development of improved absolute calibration method	August-December
Attend the 2019 APS conference	October
Design and source solid state calibration source	January - May
Test and quantify solid-state calibration method	June - July

Grant Year 3 Tasks
August 15, 2020 - August 14, 2021

Task	Period
Install solid state calibration device	August
Attend the 2020 APS conference	October
Participation in the OP2 campaign	June - August

Appendix 1: Biographical Sketches

Miklos Porkolab CURRICULUM VITAE

EDUCATION

Stanford University Ph.D., Applied Physics	1967
Stanford University M.S., Applied Physics	1964
University of British Columbia B.A.Sc., Engineering Physics	1963

APPOINTMENTS

Massachusetts Institute of Technology, Professor of Physics	1977-present
PSFC - CRPP - JET TAE Project, PI	2002-present
PCI Diagnostic on Versator II, DIII-D and C-Mod, PI	1990-present
PCI Project on Wendelstein W7-X, PI	2015-present
Plasma Science and Fusion Center, MIT, Director	1995-2014
Plasma Fusion Center, MIT, Associate Director	1990-1995
Alcator Project, Co-PI	1995-2014
Versator II program, Co-PI	1978-1985
Alcator Lower Hybrid Project, PI	1878-1988
Alcator Project, ICRF Group Leader	1990-2000
Princeton U. and Plasma Physics Laboratory,	1975-1977
Senior Research Scientist, and Lecturer with Rank of Professor	
Princeton Plasma Physics Laboratory, Research Scientist	1968-1975
Princeton Plasma Physics Laboratory, Research Associate	1967-1968
Stanford University, Research Assistant	1963-1967

RECENT PUBLICATIONS

1. P. Ennever, M. Porkolab, J. Candy, C. Staebler, M.L. Reinke, J.E. Rice, J.C. Rost, D. Ernst, J. Hughes, S.G. Baek, and Alcator C-Mod Team, "The effects of main ion dilution on turbulence in low q_{95} C-Mod ohmic plasmas and comparisons with nonlinear GYRO," Phys. Plasmas 23, 082509 (2016).

2. P. Puglia, W. Pires de Sa, P. Blanchard, S. Dorling, S.Dowson, A. Fasoli, J. Figueiredo, R. Galvao, M. Graham, G. Jones, C. Perex von Thun, M. Porkolab, L. Ruchko, D. Testa, P. Woskov, M.A. Albarracin-Manrique and JET Contributors, "The upgraded JET toroidal Alfven eigenmode diagnostic system,?? Nuclear. Fusion 56, 112020 (2016).

3. N. Tsujii, M. Porkolab, P. T. Bonoli, E.M. Edlund. P.C. Ennever, Y. Lin, J.C. Wright, S. J. Wukitch, E.F. Jaeger, D.L. Green and R.W. Harvey, "Validation of full wave simulations for mode conversion of waves in the ICRF regime with phase contrast imaging in Alcator C-Mod," Phys. Plasmas 22, 082502 (2015).

4. A. Marinoni, J. C. Rost, M. Porkolab, A.E. Hubbard, T.H. Osborne, A.E. White, D.G. Whyte, T.L. Rhodes, E.M. Davis, D.R. Ernst, and K.H. Burrell, "Characterization of density fluctuations during the search for an I-mode regime on DIII-D tokamak," Nucl. Fusion 55, 093019 (2015).

5. J. C. Rost, M. Porkolab, J. Dorris and K.H. Burrell, ?Short wavelength turbulence generated by shear in the quiescent H-mode edge on DIII-D," Phys. Plasmas 21, 062306 (2014).

6. M. Porkolab, J. Dorris, P. Ennever, C. Fiore, M. Greenwald, A. Hubbard, Y. Ma, E. Marmar, Y. Podpaly, M. L. Reinke, J. A. Rice, J. C. Rost, N. Tsujii, D. Ernst, J. Candy, G. Staebler, and R. E. Waltz, ?Transport and turbulence studies in the linear confinement regime in Alcator C-Mod," Plasma Phys. Contr. Fusion 54, 124029 (2012).

7. E. M. Edlund, M. Porkolab, G. J. Kramer, L. Lin, Y. Lin, N. Tsujii and S. J. Wukitch, ? Experimental study of reversed shear Alfvén eigenmodes during the current ramp in the Alcator C-Mod tokamak," Plasma Phys. Contr. Fusion 52, 115003 (2010).

8. E. M. Edlund, M. Porkolab, G. J. Kramer, L. Lin, Y. Lin, S. J. Wukitch, ?Phase contrast imaging measurements of reversed shear Alfvén eigenmodes during sawteeth in Alcator C-mod," Phys. Plasmas, 16, 056106 (2009).

9. L. Lin, M. Porkolab, E. M. Edlund, J. C. Rost, M. Greenwald, N. Tsujii, J. Candy, R. E.Waltz and D. R. Mikkelsen, ?Studies of turbulence and transport in Alcator C-Mod ohmic plasmas with phase contrast imaging and comparisons with gyrokinetic simulations?, Plasma Phys. Contr. Fusion 51, 065006 (2009).

10. M. Porkolab, C. Rost, N. Basse, J. Dorris, E. Edlund, L. Lin, Y. Lin and S. J. Wukitch, ?Phase contrast imaging of waves and instabilities in high temperature magnetized fusion plasmas?, IEEE Trans. Plasma Sci. 34 229 (2006).

SYNERGISTIC ACTIVITIES

- Elected External Member, Hungarian Academy of Sciences, 2016
- Hannés Alfvén Prize and Medal, European Physical Society, 2013
- Distinguished Career Award, Fusion Power Associates, 2010
- James Clerk Maxwell Prize, American Physical Society, 2009
- Simony Karoly Memorial Plaque and Prize, Hungarian Nuclear Society, 2007
- Fellow, AAAS (2005), and APS (1975)
- Chairman of the Board, Fusion Power Associates, 2000-2005
- Vice Chair (1998) and Chair (1999), American Physical Society, Plasma Physics Division
- Vice Chair, University Fusion Association, 1997
- Editor, Physics Letters A, 1991-2001
- Advisory Committees: CRPP and Faculty of Science, EPFEL (Lausanne, Switzerland), GTC Program Advisory Committee, UC Irvine; Wigner Institute of Physics, Hungary; Fusion Program, Hungarian Academy of Sciences

GRADUATE STUDENTS

Evan Davis, Hong Sio (MIT)

POSTDOCTORAL FELLOWS

Valentin Aslanyan

COLLABORATORS AND COAUTHORS OF THE LAST 48 MONTHS

Dr. Jeff Candy, General Atomics; Prof. Pat Diamond, UCSD; Prof. Jan Egedal, Univeristy of Wisconsin; Dr. Will Fox, PPPL; Dr. G. Kramer, PPPL; Dr. D. R Mikkelsen, PPPL; Dr. R. Pinsker, General Atomics; Dr. Ron Prater, General Atomics; Dr. Gary Staebler, General Atomics; Dr. R. Waltz, General Atomics

Eric Edlund CURRICULUM VITAE

EDUCATION

Massachusetts Institute of Technology Ph.D., Physics 2009
California State University, Chico B.S., Physics and Mathematics 2003

APPOINTMENTS

SUNY Cortland, Assistant Professor of Physics Aug 2017–present
Massachusetts Institute of Technology, Staff Scientist 2014–present
US DOE, Office of Fusion Energy Sciences, Research Physicist Apr–May 2015
California Polytechnic University, San Luis Obispo, Lecturer Jan–June 2013
Princeton Plasma Physics Laboratory, Associate Research Physicist 2009–2014

RECENT PUBLICATIONS

1. C. Theiler, J. L. Terry, E. Edlund, I Cziegler, R. M. Churchill, J. W. Hughes, B. Labombard, T. Golfinopoulos, "Radial localization of edge modes in Alcator C-Mod pedestals using optical diagnostics" Plasma Physics and Controlled Fusion 59, 025016 (2017).
2. A. J. Creely, A. E. White, E. M. Edlund, N. T. Howard, and A. E. Hubbard, "Perturbative thermal diffusivity from partial sawtooth crashes in Alcator C-Mod" Nuclear Fusion 56, 036003 (2016).
3. E. M. Edlund and H. Ji, "Reynolds number scaling of boundary layer Fluxes of angular momentum in Taylor-Couette experiments" Physical Review E 82, 043005 (2015).
4. E. M. Edlund and H. Ji, "Nonlinear stability of laboratory quasi-Keplerian flow" Physical Review E 89, 021004 (2014).
5. J. H. Rhoads, E.M. Edlund, H. Ji, "Effects of magnetic field on the turbulent wake of a cylinder in MHD channel flow" Journal of Fluid Mechanics 742, 446 (2014).
6. A. H. Roach, E. J. Spence, C. Gissinger, E. M. Edlund, P. Sloboda, J. Goodman, H. Ji, "Observation of a free-Shercliff-layer instability in cylindrical geometry" Physical Review Letters 108, 154502 (2012).
7. E. J. Spence, A. H. Roach, E. M. Edlund, P. Sloboda, H. Ji, "Free MHD shear layers in the presence of rotation and magnetic field" Physics of Plasmas 19, 056502 (2012).
8. E. M. Edlund, M. Porkolab, G. J. Kramer, L. Lin, Y. Lin, N. Tsujii and S. J. Wukitch, "Experimental study of reversed shear Alfvèn eigenmodes during the current ramp in the Alcator C-Mod tokamak" Plasma Physics and Controlled Fusion 52, 115003 (2010).
9. E. M. Edlund, M. Porkolab, G. J. Kramer, L. Lin, Y. Lin and S. J. Wukitch, "Observation of reversed shear Alfvèn eigenmodes between sawtooth rashes in the Alcator C-Mod tokamak" Physical Review Letters 102, 165003 (2009).
10. E. M. Edlund, M. Porkolab, G. J. Kramer, L. Lin, Y. Lin and S. J. Wukitch, "Phase contrast imaging measurements of reversed shear Alfvèn eigenmodes during sawteeth in Alcator C-Mod" Physics of Plasmas 16, 056106 (2009).

SYNERGISTIC ACTIVITIES

• Taught at Princeton University, Cal Poly (San Luis Obispo) and MIT in a range of physics courses
• Supervisor for research interns at PPPL and MIT

COLLABORATORS AND COAUTHORS OF THE LAST 48 MONTHS

S. G. Baek, MIT; P. T. Bonoli, MIT; L.-G. Böttger, IPP-Greifswald; M. Burin, CSU San Marcos; A. Creely, MIT; I. Cziegler, U. York; E. Davis, MIT; L. Delgado-Aparicio, PPPL; A. Diallo, PPPL; A. Dominguez, PPPL; P. C. Ennever, private business; D. Ernst, MIT; I. C. Faust, IPP-Garching; W. R. Fox, PPPL; E. Fredrickson, PPPL; C. Gao, private business; E. Gilson, PPPL; J. Goodman, Princeton Uni.; T. Golfinopoulos, MIT; R. S. Granetz, MIT; M. J. Greenwald, MIT; O. Grulke, IPP-Greifswald; N. T. Howard, MIT; A. E. Hubbard, MIT; J. W. Hughes, MIT; J. Irby, MIT; G. J. Kramer, PPPL; B. Labombard, MIT; S. Lazerson, PPPL; Y. Lin, MIT; A. Marinoni, General Atomics; E. S. Marmar, MIT; R. M. McDermott, IPP-Garching; D. Mikkelsen, PPPL; N. Pablant, PPPL; R. R. Parker, MIT; J. E. Rice, MIT; C. Rost, MIT; S. Shiraiwa, MIT; C. Sung, MIT; J. Terry, MIT; N. Tsujii, University of Tokyo; A. von Stech

Appendix 2: Current and Pending Support

Prof. Miklos Porkolab

Support: ☒ Current ☐ Pending
Project/Proposal Title: Interferometer Diagnostics
Source of Support: DOE
Total Award Amount: $3,796,948 Award Period Covered: 10/15/95-6/30/18
Person-Months Per Year Committed to the Project. Summer: 0.75

Support: ☒ Current ☐ Pending
Project/Proposal Title: Measurement of Helicons and Parametric Decay Waves in DIII-D with Phase Contrast Imaging
Source of Support: DOE
Total Award Amount: $840,000 Award Period Covered: 8/1/16-7/31/19
Person-Months Per Year Committed to the Project. Summer: 1.1

Support: ☒ Current ☐ Pending
Project/Proposal Title: Alcator C-Mod
Source of Support: DOE
Total Award Amount: $235,443,932 Award Period Covered: 12/1/98-9/30/17
Person-Months Per Year Committed to the Project. Summer: 0.1

Support: ☒ Current ☐ Pending
Project/Proposal Title: Fast Particle Wave Interaction and Alfven Eigenmodes in the JET Tokamak Plasma
Source of Support: DOE
Total Award Amount: $440,317 Award Period Covered: 12/23/14-3/31/18
Person-Months Per Year Committed to the Project. Summer: 0.75

Support: ☒ Current ☐ Pending
Project/Proposal Title: Phase Contrast Imaging for Wendelstein 7-X
Source of Support: DOE
Total Award Amount: $1,039,000 Award Period Covered: 8/15/15-8/14/18
Person-Months Per Year Committed to the Project. Summer 1.1

Support: ☒ Current ☐ Pending
Project/Proposal Title: Development of an Ultrahigh-bandwidth Phase Contrast Imaging System for detection of Electron scale turbulence and Gigahertz Radiofrequency Waves
Source of Support: DOE
Total Award Amount: $200,000 Award Period Covered: 9/1/17-8/31/19
Person-Months Per Year Committed to the Project. Summer: 0.7

Support: ☐ Current ☒ Pending
Project/Proposal Title: THIS PROPOSAL- Fast Particle Wave Interaction and Alfven Eigenmodes in the JET Tokamak Plasma (Renewal)
Source of Support: DOE
Total Award Amount: $556,575 Award Period Covered: 4/1/18-3/31/21
Person-Months Per Year Committed to the Project. Summer: 1.0

Support: ☐ Current ☒ Pending
Project/Proposal Title: THIS PROPOSAL- Phase Contrast Imaging for Wendelstein 7-X (Renewal)
Source of Support: DOE
Total Award Amount: $900,000 Award Period Covered: 8/15/18-8/14/21
Person-Months Per Year Committed to the Project. Summer: 1.1

Current and Pending Support
Investigator: Eric Edlund, SUNY Cortland

Support: ☒ Current ☐ Pending

Project/Proposal Title: Phase contrast Imaging for Wendelstein 7-X

Source of Support: DOE

Total Award Amount: $ 1,039,000

Award Period Covered: 8/15/2015 - 8/15/2018

Location of Project: MIT

Person-Months Per Year Committed to the Project: 12

Support: ☐ ☒ Pending

Project/Proposal Title: Phase contrast Imaging for Wendelstein 7-X (THIS PROPOSAL)

Source of Support: DOE DE-FOA-0001811

Total Award Amount (subcontract): $ 192,606

Award Period Covered: 8/15/2018 - 8/15/2021

Location of Project: SUNY Cortland

Person-Months Per Year Committed to the Project: 2

Appendix 3: References Cited

[1] V. Erckmann, F. Wagner, J. Baldzuhn, R. Brakel, R. Burhenn, U. Gasparino, P. Grigull, H. J. Hartfuß, J. V. Hofmann, R. Jaenicke, H. Niedermeyer, W. Ohlendorf, A. Rudyj, A. Weller, S. D. Bogdanov, B. Bomba, A. A. Borschegovsky, G. Cattanei, A. Dodhy, D. Dorst, A. Elsner, M. Endler, T. Geist, L. Giannone, H. Hacker, O. Heinrich, G. Herre, D. Hildebrandt, V. I. Hiznyak, V. I. Il'in, W. Kasparek, F. Karger, M. Kick, S. Kubo, A. N. Kuftin, V. I. Kurbatov, A. Lazaros, S. A. Malygin, V. I. Malygin, K. McCormick, G. A. Müller, V. B. Orlov, P. Pech, I. N. Roi, F. Sardei, S. Sattler, F. Schneider, U. Schneider, P. G. Schüller, G. Siller, U. Stroth, M. Tutter, E. Unger, H. Wolff, E. Würsching, and S. Zöpfel, "H-Mode of the W7-AS stellarator," Physical Review Letters **70** (1993) 2086.

[2] M. Greenwald, "Density limits in toroidal plasmas," Plasma Physics and Controlled Fusion **44** (2002) R27.

[3] D. A. Gates and L. Delgado-Aparicio, "Origin of tokamak density limit scalings," Physical Review Letters **108** (2012) 165004.

[4] P. Helander, C. D. Beidler, T. Bird, M. Drevlak, Y. Feng, R. Hatzky, F. Jenko, R. Kleiber, J. H. E. Proll, Y. Turkin, and P. . Xanthopoulos, "Stellarator and tokamak plasmas: a comparison," Plasma Physics and Controlled Fusion **54** (2012) 124009.

[5] K. McCormick, P. Grigull, R. Buhrenn, R. Brakel, H. Ehlmer, Y. Feng, F. Gadelmeier, L. Giannone, D. Hildebrandt, M. Hirsch, R. Jaenicke, J. Kisslinger, T. Klinger, S. Klose, J. P. Knauer, R. König, G. Kühner, H. P. Laqua, D. Naujoks, H. Niedermeyer, E. Pasch, N. Ramasubramanian, N. Rust, F. Sardei, F. Wagner, A. Weller, U. Wenzel, and A. Werner, "New advanced operational regime on the W7-AS stellarator," Physical Review Letters **89** (2002) 015001.

[6] H. J. Hartfuß, H. Maaßberg, M. Tutter, and W VII-A Team and ECRH Group, "Evaluation of the local heat conductivity coefficient by power-modulated electron cyclotron heating in the Wendelstein VII-A Stellarator," Nuclear Fusion **26** (1986) 678.

[7] U. Stroth, "A comparative study of transport in stellarators and tokamaks," Plasma Physics and Controlled Fusion **40** (1998) 9.

[8] G. A. Muller, V. Erckmann, H. Hartfuß, H. Laqua, H. Maaßberg, M. Rome, U. Stroth, and A. Weller, "Shear modification by ECCD and related confinement phenomena in W7-AS," Proceedings of the 11th Topical Conference on Radio Frequency Power in Plasmas (Palm Springs, CA) (1995).

[9] A. Dinklage, H. Maaßberg, R. Preuss, Y. A. Turkin, H. Yamada, E. Ascasibar, C. D. Beidler, H. Funaba, J. H. Harris, A. Kus, S. Murakami, S. Okamura, F. Sano, U. Stroth, Y. Suzuki, J. Talmadge, V. Tribaldos, K. Y. Watanabe, A. Werner, A. Weller, and M. Yokoyama, "Physical model assessment of the energy confinement time scaling in stellarators," Nuclear Fusion **47** (2007) 1265.

[10] P. Xanthopoulos, F. Merz, T. Görler, and F. Jenko, "Nonlinear gyrokinetic simulations of ion-temperature-gradient turbulence for the optimized Wendelstein 7-X stellarator," Physical Review Letters **99** (2007) 035002.

[11] V. Kornilov, R. Kleiber, and R. Hatzky, "Gyrokinetic global electrostatic ion-temperature-gradient modes in finite β equilibria of Wendelstein 7-X," Nuclear Fusion **45** (2005) 238.

[12] T. Görler, X. Lapillonne, S. Brunner, T. Dannert, F. Jenko, F. Merz, and D. Told, "The global version of the gyrokinetic turbulence code GENE," Journal of Computational Physics **230** (2011) 7053.

[13] F. Jenko, W. Dorland, M. Kotschenreuther, and B. N. Rogers, "Electron temperature gradient driven turbulence," Physics of Plasmas **7** (2000) 1904.

[14] H. E. Mynick, N. Pomphrey, and P. Xanthopoulos, "Optimizing stellarators for turbulent transport," Physical Review Letters **105** (2010) 095004.

[15] S. Zoletnik, M. Anton, M. Endler, S. Fiedler, M. Hirsch, K. McCormick, J. Schweinzer, and the W7-AS Team, "Density fluctuation phenomena in the scrape-off layer and edge plasma of the Wendelstein 7-AS stellarator," Physics of Plasmas **6** (1999) 4239.

[16] N. P. Basse, S. Zoletnik, P. K. Michelsen, and the W7-AS Team, "Study of intermittent small-scale turbulence in Wendelstein 7-AS plasmas during controlled confinement transitions," Physics of Plasmas **12** (2005) 012507.

[17] H. Weisen, "Imaging methods for the observation of plasma density fluctuations," Plasma Physics and Controlled Fusion **28** (1986) 1147.

[18] M. Porkolab, J. C. Rost, N. Basse, J. Dorris, E. Edlund, L. Lin, Y. Lin, and S. Wukitch, "Phase contrast imaging of waves and instabilities in high temperature magnetized fusion plasmas," IEEE Transactions on Plasma Science **34** (2006) 229.

[19] E. M. Edlund, M. Porkolab, G. J. Kramer, L. Lin, Y. Lin, and S. J. Wukitch, "Observation of Reversed Shear Alfvén Eigenmodes between Sawtooth Crashes in the Alcator C-Mod Tokamak," Physical Review Letters **102** (2009) 165003.

[20] E. M. Edlund, M. Porkolab, O. Grulke, C. Sehren, and L. Böttger, "Design of a Phase Contrast Imaging Diagnostic for the Wendelstein 7-X Stellarator," Bulletin of the American Physical Society **61** (2016) 272.

[21] E. M. Edlund, M. Porkolab, O. Grulke, A. von Stechow, and L. Böttger, "First results from the Wendelstein 7-X Phase Contrast Imaging System," Bulletin of the American Physical Society **62** (2017) 90.

[22] E. M. Edlund, M. Porkolab, G. J. Kramer, L. Lin, Y. Lin, N. Tsujii, and S. J. Wukitch, "Experimental study of reversed shear Alfvén eigenmodes during the current ramp in the Alcator C-Mod tokamak," Plasma Physics and Controlled Fusion **52** (2010) 115003.

[23] L. Lin, M. Porkolab, E. M. Edlund, J. C. Rost, C. L. Fiore, M. Greenwald, Y. Lin, D. R. Mikkelsen, N. Tsujii, and S. J. Wukitch, "Studies of turbulence and transport in Alcator C-Mod H-mode plasmas with phase contrast imaging and comparisons with GYRO," Physics of Plasmas **16** (2009) 012502.

[24] M. Greenwald, R. Boivin, P. Bonoli, C. Fiore, J. Goetz, R. Granetz, A. Hubbard, I. Hutchinson, J. Irby, Y. Lin, E. Marmar, A. Mazurenko, D. Mossessian, T. Sunn-Pedersen, J. Rice, J. Snipes, G. Schilling, G. Taylor, J. Terry, S. Wolfe, and S. Wukitch, "Studies of EDA H-mode in Alcator C-Mod," Plasma Physics and Controlled Fusion **42** (2000) A263.

[25] D. G. Whyte, A. E. Hubbard, J. W. Hughes, B. Lipschultz, J. E. Rice, E. S. Marmar, M. Greenwald, I. Cziegler, A. Dominguez, T. Golfinopoulos, N. Howard, L. Lin, R. M. McDermott, M. Porkolab, M. L. Reinke, J. Terry, N. Tsujii, S. Wolfe, S. Wukitch, Y. Lin, and the Alcator C-Mod Team, "I-mode: an H-mode energy confinement regime with L-mode particle transport in Alcator C-Mod," Nuclear Fusion **50** (2010) 105005.

[26] P. Ennever, M. Porkolab, J. Candy, G. Staebler, M. L. Reinke, J. E. Rice, J. C. Rost, D. Ernst, J. Hughes, S. G. Baek, and A. C.-M. Team, "The effects of main-ion dilution on turbulence in low q95 C-Mod ohmic plasmas, and comparisons with nonlinear GYRO," Physics of Plasmas **23** (2016) 082509.

[27] M. Porkolab, J. Dorris, P. Ennever, C. Fiore, M. Greenwald, A. Hubbard, Y. Ma, E. Marmar, Y. Podpaly, M. L. Reinke, J. E. Rice, J. C. Rost, N. Tsujii, D. Ernst, J. Candy, G. M. Staebler, and R. E. Waltz, "Transport and turbulence studies in the linear ohmic confinement regime in Alcator C-Mod," Plasma Physics and Controlled Fusion **54** (2012) 124029.

[28] K. Tanaka, L. N. Vyacheslavov, T. Akiyama, A. Sanin, K. Kawahata, T. Tokuzawa, Y. Ito, S. Tsuji-Iio, and S. Okajma, "Phase contrast imaging interferometer for edge density fluctuation measurements on LHD," Review of Scientific Instruments **74** (Mar 2003) 1633.

[29] N. Tsujii, M. Porkolab, P. T. Bonoli, Y. Lin, J. C. Wright, S. J. Wukitch, E. F. Jaeger, D. L. Green, and R. W. Harvey, "Measurements of ion cyclotron range of frequencies mode converted wave intensity with phase contrast imaging in Alcator C-Mod and comparison with full-wave simulations," Physics of Plasmas **19** (2012) 082508.

[30] E. Nelson-Melby, M. Porkolab, P. T. Bonoli, Y. Lin, A. Mazurenko, and S. J. Wukitch, "Experimental observations of mode-converted ion cyclotron waves in a tokamak plasma by phase contrast imaging," Physical Review Letters **90** (2003) 155004.

[31] K. Tanaka, C. Michael, A. L. Sanin, L. N. Vyacheslavov, K. Kawahata, S. Murakami, A. Wakasa, S. Okajima, H. Yamada, M. Shoji, J. Miyazawa, S. Morita, T. Tokuzawa, T. Akiyama, M. Goto, K. Ida, M. Yoshinuma, I. Yamada, M. Yokoyama, S. Masuzaki, T. Morisaki, R. Sakamoto, H. Funaba, S. Inagaki, M. Kobayashi, A. Komori, and L. experimental group, "Experimental study of particle transport and density fluctuations in LHD," Nuclear Fusion **46** (2006) 110.

[32] P. Xanthopoulos and F. Jenko, "Gyrokinetic analysis of linear microinstabilities for the stellarator Wendelstein 7-X," Physics of Plasmas **14** (2007) 042501.

[33] J. H. E. Proll, H. E. Mynick, P. Xanthopoulos, S. A. Lazerson, and B. J. Faber, "TEM turbulence optimisation in stellarators," Plasma Physics and Controlled Fusion **58** (2016) 014006.

[34] G. J. Kramer, B. V. Budny, R. Ellis, M. Gorelenkova, W. W. Heidbrink, T. Kurki-Suonio, R. Nazikian, A. Salmi, M. J. Schaffer, K. Shinohara, J. A. Snipes, D. A. Spong, T. Koskela, and M. A. Van Zeeland, "Fast-ion effects during test blanket module simulation experiments in DIII-D" Nuclear Fusion **51** (2011) 103029.

[35] J. C. Rost, L. Lin, and M. Porkolab, "Development of a synthetic phase contrast imaging diagnostic," Physics of Plasmas **17** (2010) 062506.

[36] O. Dendy and K. G. McClements, "Ion cyclotron emission from fusion-born ions in large tokamak plasmas: a brief review from JET and TFTR to ITER," Plasma Physics and Controlled Fusion **57** (2015) 044002.

[37] S. Shoichi, I. Makoto, Y. Yuusuke, K. Makoto, I. Yasutaka, M. Tatsuya, M. Yuichiro, Y. Takuro, M. Shinichi, K. Takayuki, K. Atsushi, S. Koji, S. Yoshiteru, W. Tsuguhiro, H. Hitoshi, and I. Tsuyoshi, "Observation of Ion Cyclotron Emission Owing to DD Fusion Product H Ions in JT-60U," Plasma and Fusion Research **5** (2010) S2067.

Appendix 4: Facilities & Other Resources

IPP-Greifswald

The Max Planck Institute für Plasmaphysik in Greifswald, Germany (IPP-Greifswald) is home to the Wendelstein 7-X Stellarator experiment and other small experiments, as well as significant theoretical plasma physics and engineering divisions.

Massachusetts Institute of Technology (MIT)

The management of research activities, which are financed through contracts with government and industry, is supported by the Office of Sponsored Programs and carried out within MIT academic departments as well as many interdepartmental centers and laboratories, such as the PSFC. The Office of the Vice President for Financial Operations is responsible for financial and business policies and procedures for sponsored research, including those designed to meet the requirements of grants and contracts. The Vice President for Financial Operations is the contracting officer of the Institute and is directly responsible for the negotiation and interpretation of sponsored research contracts and grants, and for negotiating the reimbursement of indirect costs and employee benefits. The Accounting Office reporting to the Comptroller directs the accounting for all sponsored research projects. The Office of Sponsored Programs (OSP) at MIT has the immediate responsibility for the business administration aspects of research projects sponsored by the government. OSP provides summarized terms and conditions of new and renewed research contracts to the Plasma Science and Fusion Center (PSFC) Principal Investigators and key Office of Resource Management personnel. Other chief management systems MIT provides to its research community include the Comptrollers Accounting Office; Property Office; Travel Office; Payroll Office; Purchasing Department and Accounts Payable.

The Plasma Science and Fusion Center

The Plasma Science and Fusion Center (PSFC) is one of the largest on-campus research facilities at MIT. The Director of the Center, Prof. Dennis Whyte, oversees all PSFC research activities and provides the administrative interface between the PSFC and the Department of Energy, the MIT administration, and the national and international laboratories' administration. The PSFC coordinates the basic and fusion-oriented energy research activities located at MIT in order to provide the strong intellectual and administrative leadership required throughout these research programs. It is recognized as one of the leading university laboratories in the physics and engineering aspects of plasmas. The administrative, technical and research staff of the PSFC work together to coordinate the communication and research efforts required to maintain this status.

The PSFC houses an independent machine shop, vacuum shop, electronics shop and other manufacturing capabilities. A technical staff of engineers and technicians are available, as needed, for consultation regarding the design and fabrication of new components as needed. The PSFC works very closely with faculty, staff and graduate students from affiliated MIT academic departments and laboratories, including: Physics Department, Aeronautics & Astronautics Department, Electrical,,, Engineering & Computer Science Department, Materials Science & Engineering Department,

Nuclear Engineering Department, and the Francis Bitter National Magnet Laboratory.

Computer Services

The MIT Plasma Science and Fusion Center has substantial computing resources in the form of the new PSFC@Engaging cluster. This cluster is used to run advanced RF simulation tools such as GENRAY/CQL3D, TORIC, HISTORIC, and TORLH and advanced gyrokinetic codes such as GYRO, GS2, and GENE. In addition, Python based frameworks such as ?Scope and Petra have been implemented on the cluster for managing the workflows of the RF simulation codes.

This system was designed and acquired primarily by theory researchers and staff. It consists of a 100 compute node subsystem integrated into the ?Engaging Cluster,? which is located at the Massachusetts Green High Performance Computing Center (MGHPCC) in Holyoke, Massachusetts. The PSFC subsystem has access to the 2.5 Petabyte Lustre parallel file system of the Engaging Cluster. The Lustre system and nodes are connected by a high speed, low latency Infiniband network.

The PSFC subsystem was installed simultaneously with 32 identically configure nodes for the Nuclear Science and Engineering (NSE) Department ? the NSE Department shares several students and faculty with the PSFC. Joint usages of the two partitions for large scale jobs using over 4300 compute cores enables rapid development of simulations for leadership class systems.

PSFC@Engaging Technical Description

This 100 node subsystem is connected together by a high speed, non-blocking FDR Infiniband system. This Infiniband system is capable of 14 Gb/s with a latency of 0.7 microseconds. With four channels, the effective node-to-node communication speed is 56 Gb/s or 6.4 GB/s for user applications. This network is non-blocking, thus each node has immediate access to each other node as well as to the parallel file system. Each compute node in the subsystem is configured as follows: Processors: 2 - Intel E5, Haswell-EP - 2.1GHz, 16 cores each, total 32 cores Memory: 128 GB DDR4 Local Disk: 1.0 TB The total subsystem is 3200 cores with 12.8 Terabytes of memory The individual compute nodes are very similar to the compute nodes in the ?Cori ? Phase 1? system at NERSC.

SUNY Cortland

SUNY Cortland is a New York state university and a primary-undergraduate-institution located in central New York. The SUNY Cortland Office of Research and Sponsored Programs oversees the management of research funds for projects funded by outside agencies.

The university has provided Dr. Eric Edlund with a research laboratory space and funding to establish an independent research program. This laboratory space will be established as an optics lab and equipped with safety interlock systems suitable for operation of a CO_2 laser and other sensitive optical equipment.

Appendix 5: Equipment

The vast majority of required equipment for the PCI installation at IPP-Greifswald has already been purchased. An old HgCdTe detector, similar to that used in the PCI diagnostic at W7-X but of lower performance, and its associated preamplifier can be loaned from MIT to SUNY Cortland where Dr. Eric Edlund will use it as a test stand for measurements of scattered waves in air with a CO_2 laser as a test stand for the calibration and AOM systems prior to transfer to IPP-Greifswald.

Appendix 6: Data Management Plan

This Data Management Plan (DMP) describes the elements and procedures for storing, securing and sharing data associated with the collaborative research described in this proposal.

Data Covered: This plan covers the following data

- Experimental data from local facilities
- Publications and research reports in digital form
- Information from collaborating institutions: Any data created as a product of collaborative research, including analyzed data or other research products, described in this proposal and not stored off-site and covered by that site's DMP.

Data Storage, Archival and Retention policy

Primary and Secondary Data Storage

For critical data, primary storage currently consists of a 200 TB RAID6 disk array, which will contain all user and experimental data taken from the first day of operation. Every night, any new or modified data is copied to a secondary 200 TB disk array, maintained in a separate building.

Data Backup and Archival

User files are saved monthly for 1 quarter, quarterly for first year, annually after that on TSM (Tivoli Storage Manager, a large enterprise-class automated tape library maintained by MIT). The relational databases are backed up nightly, weekly, and monthly; nightly and weekly backups are saved for 8 weeks and the monthly backups are saved permanently. All of these database backups are in turn backed up to TSM on campus. Individual desktop systems in user offices are backed up using MIT?s CrashPlan cloud service.

Long Term Data Retention Policy

All data ever acquired from experiments is stored on magnetic disk and archived as described above, which provides for 4 copies of raw data and 3-4 copies of processed data, spread over 3 separate buildings on campus.

Data Access and Sharing

Access to processed data between our collaborators will be carried out on an individual level, by e-mail or shared online folders.

Publication of Documents and Digital Data

DOE?s Office of Science has recently established a new policy for management and access to digital data created through federally funded research. The requirements refer to research products, which include both digital data and digital documents. Of particular note, the policy includes a substantially new requirement for making all research data displayed in publications resulting from the proposed research open, machine-readable, and digitally accessible to the public at the time of publication?. The phrase ?data displayed? refers specifically to figures and tables within the publication.

Open Access Data Management

The Harvard/MIT Dataverse data repository will provide a stable, long-term, open, institutional archive for the digital data required under the new rules. To meet the requirement for open-access to data, researchers create a set of data files that correspond to the figures and tables as they prepare manuscripts, along with associated metadata. We have chosen to standardize on the HDF5 file format for data in figures and plain text or Excel for tables.

Document Management

To meet differing and evolving requirements from funding agencies and from MIT, digital documents will be stored redundantly in several systems. The PSFC Library will administrate the deposit to DOE P.A.G.E.S. of required metadata and links to full text as specified by OSTI/DOE. (Per the requirements of the DOE Public Access Plan). P.A.G.E.S. will link to a full-text version of the accepted manuscript twelve months from the article publication date and then link to the VoR when and if it becomes available. Metadata accompanying the accepted manuscript, e.g., author name, journal title, and digital object identifier (DOI) for the VoR, ensures that attribution to authors, journals, and original publishers will be maintained. All curated document versions are accessible through the PSFC Library website and data repository ? these versions are considered ?published? once they have been processed and administrated through the PSFC Library document ecosystem, which includes: deposit into the PSFC local digital archive; catalogued (to include all metadata) in the PSFC Online Public Access Catalog (OPAC) which includes links to all document versions; and deposited into MIT?s DSpace. The PSFC archive, Dataverse and the MIT DSpace repository are open-access to all, within and beyond the PSFC and MIT communities, without restrictions, aside from any copyright or terms-of-use provisions that may apply to specific documents or data sets.

Appendix 7: Other Attachments

- Letter from Dr. Thomas Klinger, IPP-Greifswald